Engineering Geology 192 (2015) 113–128

Contents lists available at ScienceDirect

Engineering Geology

journal homepage: www.elsevier.com/locate/enggeo

Probabilistic assessment of liquefaction-induced lateral spreads using CPT — Focusing on the 2010–2011 Canterbury earthquake sequence

Sara Khoshnevisan [a], Hsein Juang [a], Yan-Guo Zhou [b], Wenping Gong [a,*]

[a] Glenn Department of Civil Engineering Clemson University, SC 29634-0911, USA
[b] MOE Key Laboratory of Soft Soils and Geoenvironmental Engineering, Institute of Geotechnical Engineering, Zhejiang University, Hangzhou 310058, PR China

ARTICLE INFO

Article history:
Received 18 June 2014
Received in revised form 11 March 2015
Accepted 1 April 2015
Available online 8 April 2015

Keywords:
Canterbury earthquakes
Liquefaction
Lateral spreads
Cone penetration test
Maximum likelihood analysis
Probability of exceedance

ABSTRACT

Strong earthquake events often result in liquefaction-induced ground movements such as settlements and lateral spreads that are a major cause of damage to buildings, bridges, and lifelines. This paper focuses on the subject of liquefaction-induced lateral spreads. Case histories with detailed cone penetration test (CPT) data are derived from the 2010–2011 Canterbury, New Zealand earthquake sequence and used to examine an existing empirical model for liquefaction-induced lateral spreads. The results confirmed the existence of a substantial discrepancy between the predicted and observed lateral spreads, indicating a need for improved models that consider uncertainties in the input parameters. Using a maximum likelihood analysis of the derived case histories, a new empirical probabilistic model was developed for the estimation of lateral spreads in the Christchurch, New Zealand area. Emphasis is placed on assessing the probability of exceedance of limiting displacements for design against the threat of lateral spreads. The new CPT-based probabilistic model with detailed formulations is presented along with an illustrative example. The limitations of the model are discussed.

1. Introduction

Liquefaction-induced lateral spread (or lateral displacement) often causes damage to roadways, buildings and lifelines. For example, during the 1996 Kobe, Japan earthquake, liquefaction-induced lateral spreads caused serious damages that resulted in significant destruction of the harbor facilities (Ishihara et al., 1996). The damages to buildings and roadways from such lateral spreading were also widely observed in the 1999 Kocaeli, Turkey earthquake (Cetin et al., 2004; Youd et al., 2009) and the 1999 Chi-Chi, Taiwan earthquake (Chu et al., 2006). The most recent examples of lateral spreads include the 2007 Niigata, Japan earthquake (Watanabe et al., 2007), the 2008 Wenchuan, China earthquake (Cao et al., 2011), the 2010 Maule, Chile earthquake (Bertalot et al., 2013), the 2010–2011 Christchurch, New Zealand earthquakes (Bowen et al., 2012; Cubrinovski et al., 2012a; Haskell et al., 2013), and the 2011 Tohoku, Japan earthquake (Ishihara et al., 2011; Yasuda et al., 2012).

This paper focuses on the lateral spread cases derived from the recent Christchurch, New Zealand earthquakes, in which widespread soil liquefaction occurred in the September 4, 2010 ($M_w = 7.1$) and the February 17, 2011 ($M_w = 6.2$) earthquake events (Tonkin and Taylor Ltd, 2013). In both of these events, the most severe damage to houses and bridges was often associated with liquefaction-induced lateral spreads (Bowen et al., 2012). For these case histories, the soil profile and conditions were mostly characterized with cone penetration testing (CPT). In this paper, the authors seek to i) document the case histories in a readily usable tabular form, and ii) examine the existing empirical models for lateral spread predictions.

Many investigators have contributed to the development of the empirical models for the estimation of lateral spreads (e.g., Hamada, 1987; Bartlett and Youd, 1995; Rauch, 1997; Shamoto et al., 1998; Bardet et al., 1999; Rauch and Martin, 2000; Youd et al., 2002; Zhang et al., 2004; Goh and Zhang, 2014). These models range in sophistication from simple models that involve only two parameters, thickness of the liquefied layer and ground slope, to more comprehensive models that involve multiple parameters such as moment magnitude, the distance to the source, the free field ratio, the thickness of liquefied layer, the fine content, and the median particle size. Of these models, that developed by Bartlett and Youd (1995) and updated in Youd et al. (2002), referred to herein as the Youd model, is the most widely used in practice. Since its publication, the Youd model, which generally yields conservative estimates of liquefaction-induced lateral spreads, has been examined by a number of investigators using the more recent field case histories (e.g., Cetin et al., 2002; Zhang and Zhao, 2005; Chu et al., 2006; Bowen et al., 2012; Kang et al., 2013; Robinson et al., 2013; Goh and Zhang, 2014).

While the Youd model is most widely used in practice, it requires Standard Penetration Test (SPT) data that is less available in many post-event field investigations (e.g., Robinson et al., 2013). In many parts of the world, the Cone Penetration Test (CPT) has become the in situ test of choice for engineers engaged in site characterization work.

* Corresponding author.
E-mail address: tumugwp2007@gmail.com (W. Gong).

http://dx.doi.org/10.1016/j.enggeo.2015.04.001
0013-7952/

To this end, the authors focused on the use of CPT for assessing liquefaction-induced lateral spreads, which is considered appropriate since an overwhelming majority of the post-event characterization of sites in Christchurch area were conducted using CPT. Although use of SPT–CPT correlations to convert the CPT data into the parameters that are required in the Youd model, such as the fines content and the median grain size, has been reported (e.g., Bowen et al., 2012; Robinson et al., 2013), the procedure introduces an additional layer of uncertainties. To this end, the model developed by Zhang et al. (2004) for liquefaction induced lateral spread is first assessed using the case histories derived from the recent Canterbury, New Zealand earthquakes. Then, the Zhang et al. (2004) model, which is a deterministic model, is modified into a probabilistic model based on the maximum likelihood analysis that considers the effect of the probability of liquefaction.

2. Review of the Zhang model for liquefaction-induced lateral displacement

The main component of the Zhang et al. (2004) model is the Lateral Displacement Index (*LDI*), which is an integration of the maximum cyclic shear strain (γ_{max}) over depth, defined as follows:

$$LDI = \int_0^{Z_{max}} \gamma_{max}\, dz \tag{1}$$

where Z_{max} is the maximum depth below all the potential liquefiable layers (in this study, Z_{max} is set at 20 m, the depth limit adopted in the definition of the liquefaction potential index is developed by Iwasaki et al. (1982)).

The integration of the maximum cyclic shear strain (γ_{max}) over depth was also previously adopted in the lateral spread model developed by Shamoto et al. (1998) based on an extensive experimental endeavor. In the Zhang model, however, the result of such integration is expressed as *LDI*, an index that is then used for computing the lateral displacement (*LD*):

For cases of gently sloping ground without a free face ($0.2\% < S < 3.5\%$):

$$LD = (S + 0.2) \cdot LDI. \tag{2}$$

For level ground with a free face ($4 < L/H < 40$):

$$LD = 6\,(L/H)^{-0.8} \cdot LDI \tag{3}$$

where *S* is the ground slope, *L* is the horizontal distance from the toe of a free face to the site, and *H* is the elevation difference between the level ground surface and the toe of a free face, as illustrated in Fig. 1.

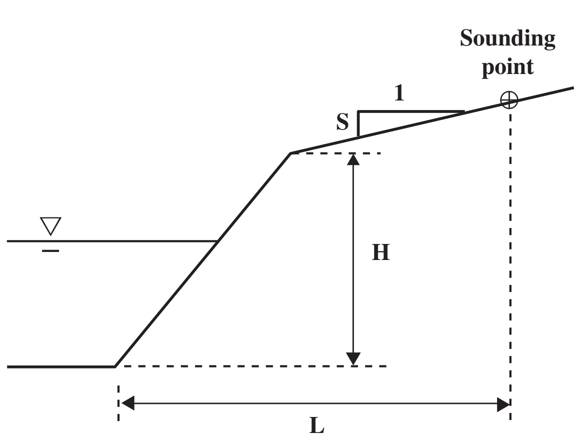

Fig. 1. Schematic diagram of lateral spread parameters (*L*, *H*, and *S* (%)).

The maximum cyclic shear strain (γ_{max}) was initially presented as a function of relative density (D_r) and factor of safety against the initiation of liquefaction (*FS*), based on the work of Ishihara and Yoshimine (1992). The mathematical expressions of the curves in a chart developed by Zhang et al. (2004) were presented in a set of 13 equations. They also introduced a correlation between D_r and the normalized CPT tip resistance corrected for effective overburden stresses, q_{c1N} (Zhang et al., 2004). Thus, γ_{max} can be evaluated based on *FS* and q_{c1N}. By considering the effect of grain characteristics, Zhang et al. (2004) suggested that the chart can also be used with two input parameters, *FS* and the clean sand equivalence of q_{c1N}, which is denoted as $q_{c1N,cs}$. Thus, a function in the form of $\gamma_{max} = f(FS, q_{c1N,cs})$ can be established. Fig. 2 shows a chart that is transformed from the one presented in Zhang et al. (2004), in which γ_{max} is computed based on *FS* and $q_{c1N,cs}$.

It should be noted that from a physical point of view, the duration of shaking (which is directly correlated to magnitude) is likely to have stronger influence on lateral displacement than on liquefaction triggering. Thus, the Zhang model, by formulating the lateral displacements as a function of geometric parameters and *FS* against liquefaction triggering, might not capture the complete effect of the magnitude. As the Zhang model is used in this study as a building block to create a probabilistic model, this limitation is inherited in the proposed model. Although this limitation is recognized, the concern is lessened with two measures: first, the magnitude effect on the lateral displacement is actually considered to some extent through the use of *FS* as an input variable; second, in the proposed model, described later, the possible model error on the predicted lateral displacement resulted from this possible magnitude effect is calibrated with field observations, and is accounted for indirectly.

In this study, a mathematical expression is further developed to represent the chart shown in Fig. 2. The maximum cyclic shear strain γ_{max} can be computed as follows:

$$\gamma_{max} = \exp[p \cdot FS + q] \tag{4}$$

where the intermediate parameters *p* and *q* are computed as:

$$p = \begin{Bmatrix} -1.246\left[\dfrac{100}{q_{c1N,cs}}\right]^3 + 4.421\left[\dfrac{100}{q_{c1N,cs}}\right]^2 - 6.626\left[\dfrac{100}{q_{c1N,cs}}\right] + 0.378 & \text{for } FS \geq 1 \\ -3.560\left[\dfrac{100}{q_{c1N,cs}}\right]^3 + 4.08\left[\dfrac{100}{q_{c1N,cs}}\right]^2 - 4.039\left[\dfrac{100}{q_{c1N,cs}}\right] - 0.122 & \text{for } FS < 1 \end{Bmatrix} \tag{5}$$

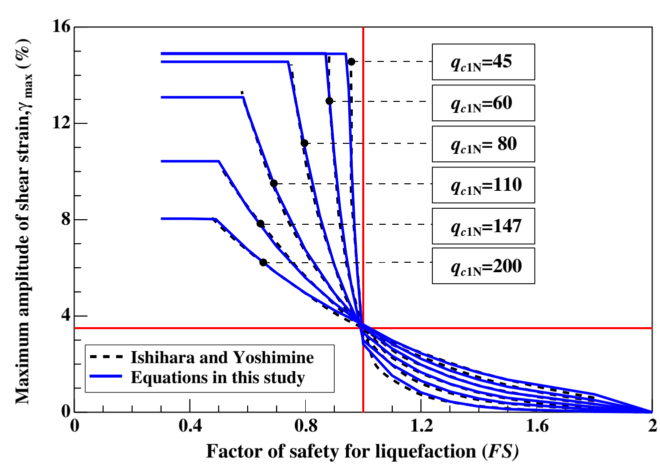

Fig. 2. Relationship between the maximum cyclic shear strain and the factor of safety for different relative densities for clean sands (based on data presented in Ishihara and Yoshimine, 1992 and modified from the chart by Zhang et al., 2004).